



Development of flexible supercapacitors with coplanar integrated multi-walled carbon nanotubes/textile electrode and current collectors

Lihong Jiang¹ , Hong Hong¹, Jiyong Hu^{1,2,*} , and Xiong Yan^{1,*}

¹ Shanghai Collaborative Innovation Center of High Performance Fibers and Composites, College of Textiles, Donghua University, Shanghai 201620, China

² Key Laboratory of Textile Science & Technology, Ministry of Education, Donghua University, Shanghai 201620, China

Received: 1 December 2021

Accepted: 5 January 2022

Published online:
22 January 2022

© The Author(s), under exclusive licence to Springer Science+Business Media, LLC, part of Springer Nature 2022

ABSTRACT

Textile-based supercapacitors are promising flexible energy storage device that can provide stable power supply for wearable electronic devices. Herein, solid-state textile-based coplanar supercapacitors have been prepared by utilizing the cost-effective multi-walled carbon nanotubes (MWCNTs) as integrated electrodes and current collectors. The integrated electrodes are fabricated with facile screen-printing process and show great potential of mass production. By optimizing the concentration of MWCNTs ink, porous and uniform conductive electrode network is formed on fabric substrate, which provide more active sites for electrolyte ions adsorption. The textile-based coplanar supercapacitors show great capacitive behavior and gravimetric specific capacitance of 26.4 F g^{-1} at scan rate of 10 mV s^{-1} . Moreover, there is no significant change on the electrochemical performance of textile-based coplanar supercapacitor under dynamically bending with relatively high strain rate of $20\% \text{ s}^{-1}$, which demonstrates excellent flexibility and electrochemical stability. It provides an important strategy for the large-scale application and development of flexible supercapacitors.

1 Introduction

Wearable electronic devices have been widely applied in the fields of medical care [1–3], communications [4, 5], aerospace [6, 7], etc. The development of flexible energy storage systems which can supply stable energy for those wearable electronic devices have attracted more and more attention. Due to the

advantages of high power density, long cycle life, wide range of operating temperature, and green manufacturing process [8, 9], supercapacitors are considered to have broad application prospects in the fields of flexible energy storage and wearable electronic devices. Supercapacitors are usually composed of electrodes, current collectors, electrolytes, separators, and encapsulation materials, which are usually

Address correspondence to E-mail: hujy@dhu.edu.cn; yaxi@dhu.edu.cn

configured in a sandwiched [10–12] or coplanar structure [13–15]. The sandwiched configuration is widely adopted in traditional bulk supercapacitors and recent flexible supercapacitors because of simple design and low internal resistance [16]. Xu et al. [17] assembled a flexible sandwiched symmetric supercapacitor by stacking the MWCNTs fabric-based electrodes and solid-state electrolyte. The specific capacitance of supercapacitor is 16.4 mF cm^{-2} at 1 mA cm^{-2} . However, the sandwich structure will significantly increase thickness and volume of supercapacitor, thereby reducing the specific capacitance and energy density of device [16]. Moreover, the layered electrodes would be in states of tensile and compressive stresses under flexing, and displacements between different layers of sandwiched capacitors are commonly observed, which is unfavorable for energy storage process and stability of supercapacitors. [18] By contrast, the coplanar configuration of supercapacitors could alleviate or eliminate the undesirable displacements and improve mechanical flexibility and electrochemical stability. [19] Meanwhile, coplanar supercapacitor can be easily connected in series or parallel and integrated with electronic devices through pattern design [20, 21], which greatly improve the integration and flexibility of energy storage devices. In addition, the configuration and fabrication process of coplanar supercapacitors are easily applied on industrial roll-to-roll manufacturing process and realize mass production of flexible energy storage devices [22].

Carbon nanomaterials, as a representative electrode material for flexible supercapacitors, have attracted extensive interests because of their excellent physicochemical properties. [23] Among them, carbon nanotubes (CNTs) have excellent mechanical and physical properties, electrical conductivity, chemical stability, and show great applications prospect in flexible supercapacitors [24, 25]. As an electrical double-layer capacitor material, it is necessary to increase the mass loading of carbon nanotubes to increase the energy density. However, due to the lack of chemical bonds between the current collectors and CNTs electrode materials [26], the excess loading of active materials may lead to delamination, capacity attenuation, and poor flexibility [27]. Therefore, the manufacturing strategy of integrating electrodes and current collectors not only can eliminate the interface between current collectors and electrodes [28], but also reduce the mass of energy storage device and

promote stability, flexibility, and energy density with simplified structure. Kaempgen et al. [28] sprayed the aqueous dispersion of single-walled carbon nanotubes (SWCNTs) on polyethylene-terephthalate (PET) film substrates to fabricate flexible electrodes. The SWCNTs conductive network serving as both electrodes and charge collectors. The energy density and power density of supercapacitor assembled with aqueous gel electrolytes are 6 Wh kg^{-1} and 23 kW kg^{-1} , respectively. Hu et al. [29] coated SWCNTs ink on the surface of cotton fabric by dipping and drying method. The conductive textiles with SWCNTs coating were used as both charge storage electrodes and current collectors. It was combined with fabric separator and LiPF₆ electrolyte to assemble flexible supercapacitor. The specific capacitance of supercapacitor is 62 F g^{-1} at 1 mA cm^{-2} . At present, most CNTs-based supercapacitors with integrated electrodes and current collectors utilized SWCNTs and aqueous electrolytes due to the low resistance of SWCNTs and high ionic conductivity of aqueous electrolytes. However, the high cost of SWCNTs makes it unable to meet the requirement of industrial production [30], and liquid electrolytes will cause safety issues such as leakage [31]. Therefore, utilizing the cost-effective multi-walled carbon nanotubes (MWCNTs, production cost is nearly 500 times lower than that of SWCNTs) [32] to prepare quasi-solid-state flexible supercapacitors is a preferred solution in the large-scale development of flexible energy storage devices.

In this work, the cost-effective coplanar flexible supercapacitor based on MWCNTs is fabricated through integrating electrodes and current collectors. The integrated MWCNTs/textile electrodes with excellent conductivity and electrochemical performance are prepared by optimizing the concentration of MWCNTs ink. The conductive ink is printed on cotton fabric through facile screen-printing process, and the MWCNTs/cotton fabric simultaneously serve as charge storage electrodes and current collectors. Combining with gel polymer electrolyte, the flexible supercapacitor was assembled, and the electrochemical performance, flexibility, and stability under initial state and dynamic bending cycles was investigated.

2 Materials and methods

2.1 Materials

MWCNTs (10–30 μm in length and 10–20 nm in outer diameter) were purchased from Nanjing XFNANO Materials Tech Co., Ltd., China. N-Methyl pyrrolidone (NMP) and ethanol absolute were purchased from Sinopharm Chemical Reagent Co., Ltd., China. Thermoplastic polyurethanes (ester based TPU, Elastollan 1185 A) was purchased from BASF, German. The defoamer (BYK-052 N), purchased from BYK company, was used to eliminate the bubbles in conductive ink, so that the MWCNTs could distribute uniformly in the fabric-based electrodes. The cotton woven fabric (yarn linear density is 14.58 tex, warp and weft yarn density are 133*72 per 10 cm) was provided by Changzhou Huijin Textile Co. Ltd., China.

2.2 Preparation of MWCNTs conductive ink

The TPU pellets with different concentration (as shown in Table 1) were dissolved in NMP solvent in a beaker, and stirred (magnetic stirrer, Shanghai Meiyongpu Instrument Manufacturing Co., Ltd., Ching) at 4 $^{\circ}\text{C}$ and 350 rpm for 60 min. According to previous studies [33], 5 wt% MWCNTs can form a complete and continuous conductive network after screen printing, so 5 wt% MWCNTs and defoamer were added to the polymer matrix and continue stirring for another 60 min. To disperse the conductive fillers uniformly, the mixed solution was treated with ultra-sonication (Q500 Sonicator, Qsonica L.L.C, USA) for 15 min, and the MWCNTs conductive inks were obtained, the preparation process is shown in Fig. 1.

Table 1 Formulation of MWCNTs conductive inks

Ingredients(wt %)	Ink-1	Ink-2	Ink-3	Ink-4
NMP	79.5	84.5	89.5	92
TPU	15	10	5	2.5
MWCNTs	5	5	5	5
BYK-052 N	0.5	0.5	0.5	0.5

2.3 Preparation of screen-printed fabric electrodes

Screen printing is one of the most promising methods for fabricating flexible electrodes, owing to its advantages of cost-effectiveness, simplicity, and the ability of printing customized patterns. [34] Before screen printing, the cotton fabrics were immersed in ethanol for 30 min followed by rinsed thoroughly with deionized water to remove impurities, then the fabrics were dried in an oven at 40 $^{\circ}\text{C}$. A desktop screen printer (Shenzhen Kaimao Mechanical and Equipment Factory, China) was used to coat the MWCNTs conductive slurry on cotton fabrics. During screen-printing process, the angle between squeegee and screen was 85 $^{\circ}$ and the printing speed was 15.0 cm s^{-1} . After screen printing, the textiles were dried and cured in oven at 80 $^{\circ}\text{C}$ for 30 min to remove the solvent in conductive ink and promote the formation of stable conductive networks.

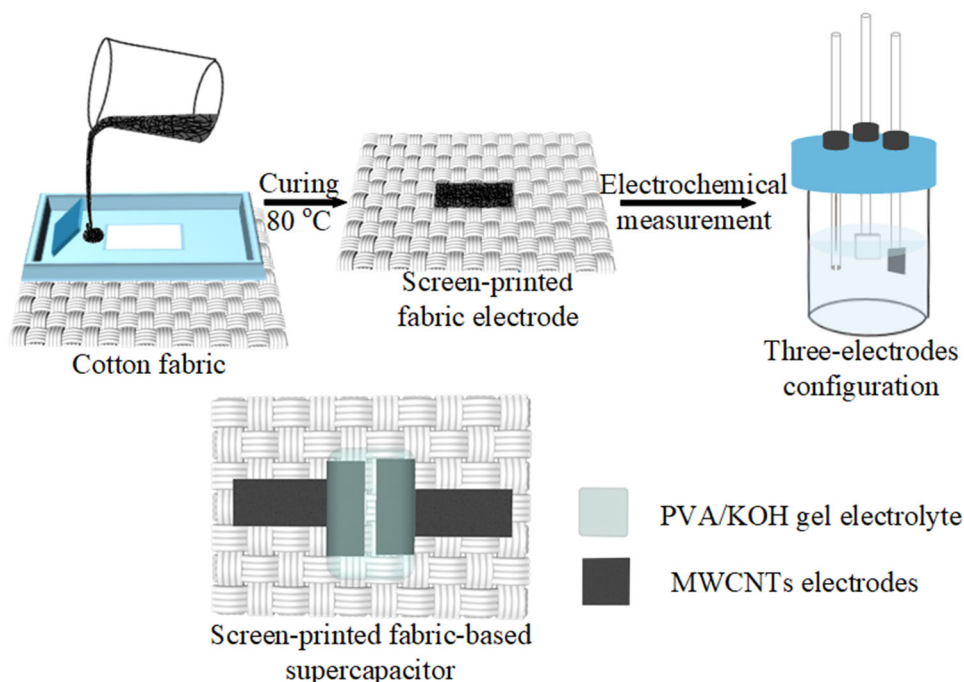
2.4 Fabrication of flexible textile-based MWCNTs supercapacitors

To assemble the textile-based supercapacitor, the positive and negative electrodes were firstly screen-printed on cotton woven fabric. After curing at 80 $^{\circ}\text{C}$ for 30 min, the fabric electrodes were coated with gel electrolyte followed by drying at room temperature for 4 h. The polyvinyl alcohol/ potassium hydroxide (PVA/KOH) gel electrolyte was prepared by adding 3 g PVA to 30 ml deionized water, and stirred at 80 $^{\circ}\text{C}$ until the solution became clear. 3 g KOH was added to 10 ml deionized water and stirred at room temperature. Then the KOH solution was added dropwise to the PVA solution and continually stirred for 1 h. The fabrication process and configuration of fabric-based supercapacitor is shown in Fig. 1.

2.5 Surface morphology and physical characterization

Field emission scanning electron microscopy (FESEM, SU8010, Hitachi Ltd., Japan) was used to observe the morphology of fabric substrates and fabric electrodes. According to the AATCC 76-2005 test method (electrical surface resistivity of fabrics), digital multi-meter (901, PROVA Instruments Inc., USA) and a pair of copper clips were employed to

Fig. 1 Schematic diagram of the fabrication process of screen-printed fabric electrodes and fabric-based supercapacitor



measure the electrical resistance of conductive fabric electrodes.

2.6 Electrochemical characterization and flexibility evaluation

The electrochemical performance of screen-printed fabric electrodes was characterized by electrochemical workstation (CHI 660D, Shanghai Chenhua Instrument Co., Ltd.) in a standard three-electrodes configuration. The fabric electrodes were cut into 1 cm² and used as working electrode, the Ag/AgCl electrode and platinum foil were used as reference electrode and the counter electrode, respectively, and the electrolyte is 2 M KOH solution. Cyclic voltammetry (CV) and galvanostatic charge and discharge (GCD) tests were performed in a potential window of -0.8 to 0.2 V. According to the reference [17], electrochemical impedance spectroscopy (EIS) was performed in the frequency range of 0.1 to 1 MHz with 5 mV amplitude.

CV and GCD measurements were performed to textile-based supercapacitors in a standard two-electrode system using electrochemical workstation (CHI 660D). The CV curves were obtained at scan rates of 10, 20, 50, 100, 200, and 500 mV s⁻¹, and the GCD curves were acquired at current density of 0.19, 0.26, 0.32, 0.64, 0.96 A g⁻¹. Electrochemical impedance

spectroscopy (EIS) was carried out in the frequency range of 0.1 Hz to 1 MHz with 5 mV amplitude.

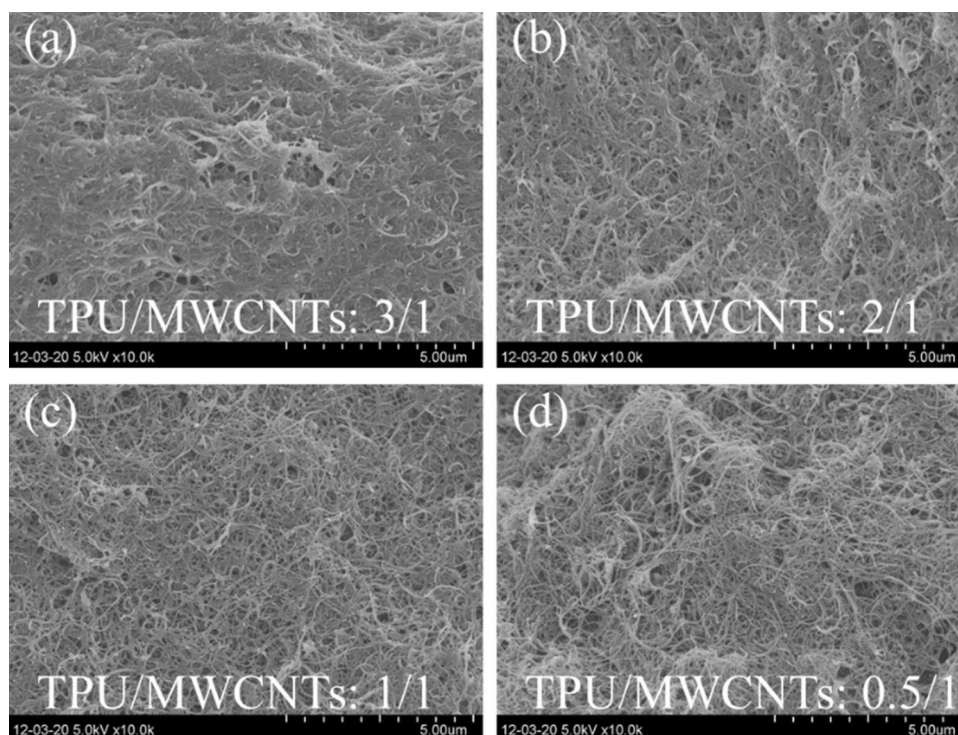
For flexibility evaluation of supercapacitors, the textile-based supercapacitor was clamped on a universal material testing machine for cyclic bending-releasing process. The bending chord length is 6 mm (60% bending strain), which is the maximum bending length under the premise that anode and cathode are not in contact. The strain rate of bending-releasing process is set to 20% s⁻¹ (speed of 2 mm s⁻¹), which is higher than some references (2–5% s⁻¹) [35, 36] and has more practical significance. The textile-based supercapacitor is connected to the electrochemical workstation (CHI 660D), and the electrochemical measurements of the fabric capacitor was performed through two-electrode configuration under dynamic bending-releasing cycles.

3 Results and discussion

3.1 The surface morphology of fabric electrodes

Figure 2 shows the surface morphology of fabric electrodes screen-printed with Ink-1 to Ink-4, respectively. It can be seen that more carbon nanotubes are exposed as the proportion of TPU in the MWCNTs ink decreases (from Fig. 2a and d). And

Fig. 2 SEM images of fabric electrodes screen-printed with different MWCNTs inks. **a** Ink-1, **b** Ink-2, **c** Ink-3, **d** Ink-4



the uniformly distributed and microscopic porous network structure was formed. The porous structure will facilitate the adsorption and desorption of electrolyte ions [36]. However, comparing Fig. 2c and d, it can be seen that when the proportion of TPU continues to decrease from 5 to 2.5 wt%, carbon nanotubes were seriously entangled and agglomerated due to the strong Van der Waals force [26]. The uneven distribution of carbon nanotubes will undoubtedly affect electrical conductivity and electrochemical performance of the fabric electrodes.

3.2 The electrical conductivity of fabric electrodes

The sheet resistance and MWCNTs mass loading of fabric electrodes prepared by screen printing with four MWCNTs inks is shown in Fig. 3a. It can be seen that the sheet resistance of screen-printed fabric electrodes gradually decreases as the increase of MWCNTs mass loading. This is because the increase of MWCNTs and decrease of TPU binder exposes more carbon nanotubes, making it easily contact with adjacent carbon nanotubes and form complete and continuous conductive network. However, although the MWCNTs content continues to increase (from

0.59 to 0.64 mg cm⁻²) when the formulation of MWCNTs ink changed from Ink-3 to Ink-4, the sheet resistance of fabric electrodes slightly increased. It is mainly because a sufficiently complete conductive network has been formed in Ink-3, and the serious agglomeration arouse in Ink-4 electrode (Fig. 2d) affect the uniformity and conductivity of conductive network. Although the sheet resistance of Ink-3-based fabric electrode is not as low as that of some published works which utilizing SWCNTs as active materials[28, 29, 37–39], the resistance is lower than many MWCNTs-based fabric electrodes[17, 32, 40–42], as is compared in Fig. 3b.

3.3 The electrochemical performance of fabric electrodes

Figure 4a shows the cyclic voltammetry curves of screen-printed fabric electrodes with scan rates of 50 mV s⁻¹ in a voltage window of -0.8 V to 0.2 V. It can be seen that the fabric electrodes screen-printed with four different MWCNTs ink all present quasi-rectangular shapes, indicating that the fabric electrodes have ideal and good capacitive performance. Comparing the area enclosed by CV curves of four fabric electrodes, it can be seen that as the proportion

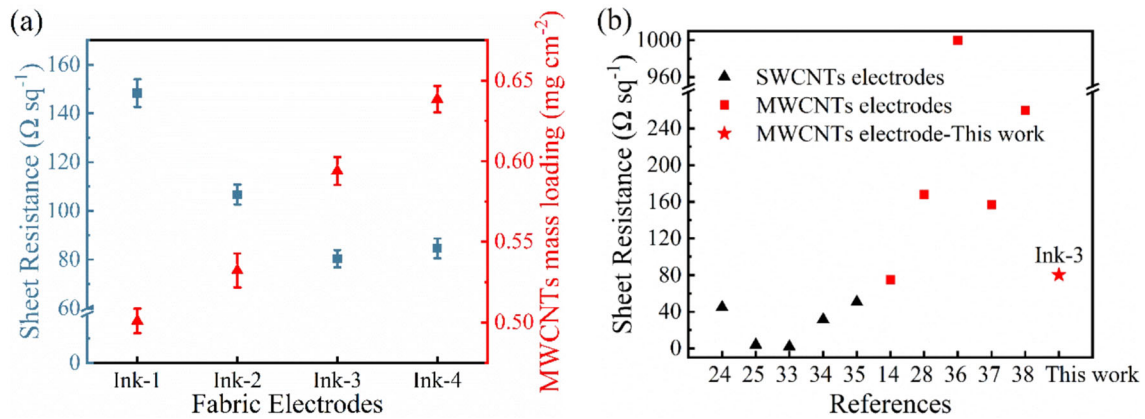


Fig. 3 a Sheet resistance and MWCNTs mass loading of fabric electrodes screen-printed with Ink-1 to Ink-4 MWCNTs inks. b Comparison of sheet resistance of fabric electrodes using carbon nanotubes in this work and other published work

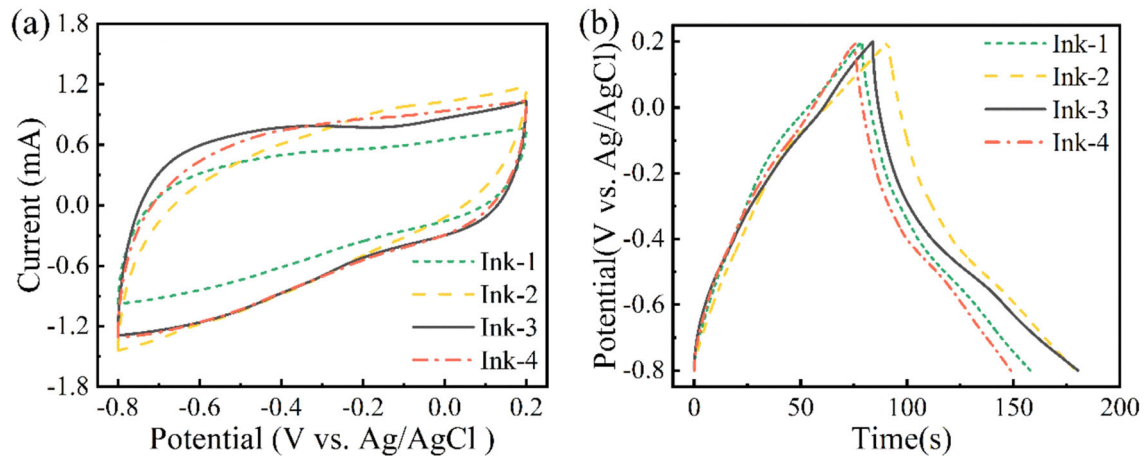


Fig. 4 a CV curves and b GCD curves of fabric electrodes screen-printed with Ink-1 to Ink-4

of MWCNTs increases (from Ink-1 to Ink-4), the area of the CV curve gradually increases, indicating that the fabric electrodes have higher capacitance. This is because a high proportion of MWCNTs can form a microscopic porous structure, as shown in Fig. 2c and d, which is conducive to the adsorption and contact between active electrode materials and the electrolyte ions [36, 43], thereby forming more active sites of electric double-layer capacitance (EDLC).

The galvanostatic charge–discharge curves of screen-printed electrodes at current density of 0.5 A g^{-1} is shown in Fig. 4b. The discharge plots of these four screen-printed fabric electrodes are almost linear and symmetrical, revealing the ideal capacitive behavior and excellent reversibility. According to the GCD curves and capacitance calculation equation [44], the specific capacitance of fabric electrodes can be calculated, as shown in Table 2. Among these four

fabric electrodes, the Ink-3 electrode shows the highest gravimetric and areal specific capacitances, which are 48.2 F g^{-1} and 29.0 mF cm^{-2} , respectively. This is mainly attributed to the formation of uniform and microporous MWCNTs network in Ink-3 electrode layer, which can be clearly seen in Fig. 2c. More carbon nanotubes are exposed when the proportion of binder decrease, which could provide more active sites for absorption of electrolyte ions and improve electric double-layer capacitance (EDLC)[36]. However, when the content of binder continually decreases (from Ink-3 to Ink-4), MWCNTs obviously agglomerate together, as shown in Fig. 2d, thereby blocking many active sites and leading to a decrease in capacitance. It is noted that the slight hump around -0.6 V in Fig. 4a is ascribed to the relationship between the pore size of carbon nanotubes and ions sizes in KOH electrolyte. According to the CRC

Table 2 Gravimetric and areal specific capacitances of screen-printed fabric electrodes

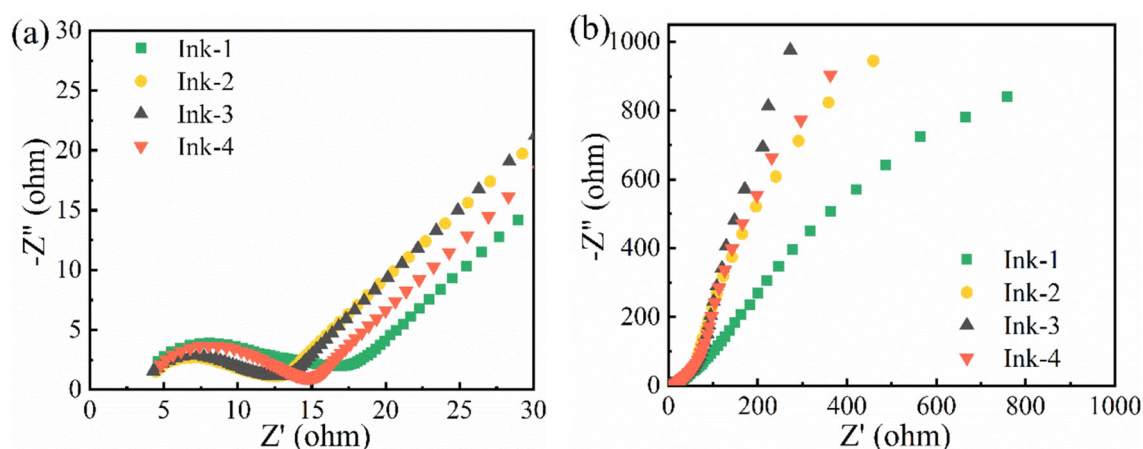
Fabric electrodes	Gravimetric capacitances ($F\ g^{-1}$)	Areal capacitances ($mF\ cm^{-2}$)
Ink-1	39.6	19.9
Ink-2	43.9	23.0
Ink-3	48.2	29.0
Ink-4	36.6	23.5

Handbook of Chemistry and Physics (95th) [45], the radii of K^+ and OH^- are 0.138 nm and 0.152 nm, respectively. The different sizes of anion and cation ions make them have different accessibility for insertion and adsorption on the pore of carbon nanotube, which results in the slight hump in CV and GCD curves.[46, 47].

The resistive behavior of fabric electrodes screen-printed with different inks were investigated through the electrochemical impedance spectroscopy (EIS). Figure 5 shows the Nyquist plots of different screen-printed fabric electrodes. The Nyquist plot generally includes three parts as follows: a steep slope in the low-frequency region, a 45° Warburg region, and a semicircle curve at high frequency. [48, 49] The enlarged image of Nyquist plot captured in the high-frequency region is shown in Fig. 5a. The diameter of the semicircle arc is related to the charge transfer resistance (R_{ct}) of electrolyte and electrode interface [50]. It can be seen that the charge transfer resistance of Ink-2 and Ink-3 fabric electrodes are smaller than Ink-4 and Ink-1 electrodes. The excellent resistive behavior is mainly attribute to the uniform conductive network (Fig. 2c) and lowest sheet resistance of Ink-3 fabric electrode (Fig. 3). The slope at low frequency is related with the capacitive behavior of the electric double-layer capacitor (EDLC) [51]. It is

obviously observed that the Ink-3 fabric electrode nearly maintains a vertical line in the low-frequency region (Fig. 5b), revealing better capacitive behavior than other electrodes. In contrast, the Ink-1 fabric electrode exhibits the largest charge transfer resistance, lowest slope, and poor capacitance behavior. This is mainly due to the relatively high proportion of TPU binder in Ink-1 electrode. As shown in Fig. 2a, the MWCNTs are coated with many binders, which is not conducive to the adsorption of electrolyte ions and the diffusion and transfer of electrons inside the electrode.

In general, Ink-3 fabric electrode has the greatest conductivity and electrochemical performance. This is mainly attributed to the porous microstructure and uniform conductive network formed in Ink-3 fabric electrode, as shown in Fig. 2c. The porous microstructure can provide more active sites for the adsorption of electrolyte ions and improve the EDLC capacitance. Moreover, the uniform and complete conductive network formed by carbon nanotubes is beneficial to charge transfer, which could reduce the internal resistance of fabric-based electrode. Therefore, Ink-3 was used for the subsequent printing of anode and cathode and the assembly of fabric-based coplanar supercapacitors.

**Fig. 5** The **a** enlarged image and **b** overall image of Nyquist plots for fabric electrodes screen-printed with Ink-1 to Ink-4

3.4 The electrochemical performance of fabric-based coplanar supercapacitor

Electrochemical properties of screen-printed coplanar supercapacitors were evaluated by CV, GCD, and EIS techniques, in two-electrode system. Figure 6a shows the CV curves of fabric supercapacitor device in the potential window of 0 to 0.8 V, acquired at scan rates varying from 10 to 500 mV s^{-1} . It can be observed that the CV curves of fabric-based supercapacitor maintains a symmetrical shape at a wide range of scan rates, indicating that the fabric-based coplanar supercapacitor has good capacitive performance. The gravimetric and areal specific capacitance calculated from the CV curve are 26.4 F g^{-1} and 13.8 mF cm^{-2} (at scan rate of 10 mV s^{-1}), respectively, which surpass many other reported flexible fabric/membrane-based supercapacitors composed of carbon nanotubes, as shown in Table 3. The GCD curves of fabric-based supercapacitor is shown in Fig. 6b. It can be seen that the GCD curves are almost linear and symmetrical at different current densities, which reveals the ideal capacitive behavior and excellent reversibility of supercapacitor device. According to the GCD curves, the gravimetric and areal specific capacitance of the fabric-based supercapacitor were calculated to be 6.2 F g^{-1} and 3.3 mF cm^{-2} at current density of 0.19 A g^{-1} , respectively.

The EIS test was further performed to investigate the internal and charge transfer resistance of fabric-based supercapacitor, and the Nyquist plot within a frequency range of 0.1 Hz to 100 kHz is shown in Fig. 7. It can be seen that the plot of screen-printed

fabric-based supercapacitor in low frequency is nearly vertical, indicates the excellent capacitive behavior of the fabricated supercapacitor. The intercept of the Nyquist plot on the real axis is related to the equivalent series resistance (ESR) [54], which is nearly about 292.3Ω for the prepared supercapacitor. Compared with single fabric electrodes, the equivalent series resistance of supercapacitors is much larger. This is because the equivalent series resistance in supercapacitor includes the electrode resistance, electrolyte resistance, and the interfacial resistance between electrolyte and electrodes. [51] Aqueous electrolyte (2 M KOH solution) was used in the measurement of single fabric electrode, and its electrolyte resistance and interfacial resistance between electrolyte and electrodes are significantly lower than the PVA/KOH solid-state gel polymer electrolyte [55]. Due to the addition of binder into the MWCNTs inks and the relatively low conductivity compared with SWCNTs, the resistance performance still cannot compete with some of supercapacitors based on SWCNTs electrodes and binder-free electrodes. [28, 56, 57] However, the screen-printed fabric supercapacitors exhibit excellent capacitive behavior and cost-effectiveness, which make them have great potential for large-scale applications on wearable electronic devices. And the internal resistance of screen-printed fabric-based supercapacitors can be further reduced by optimizing the conductivity of polymer gel electrolyte, and the structure of electrodes. As shown in Fig. 7b, the capacitance retention is over 90.0% after 2000 charging/discharging cycles,

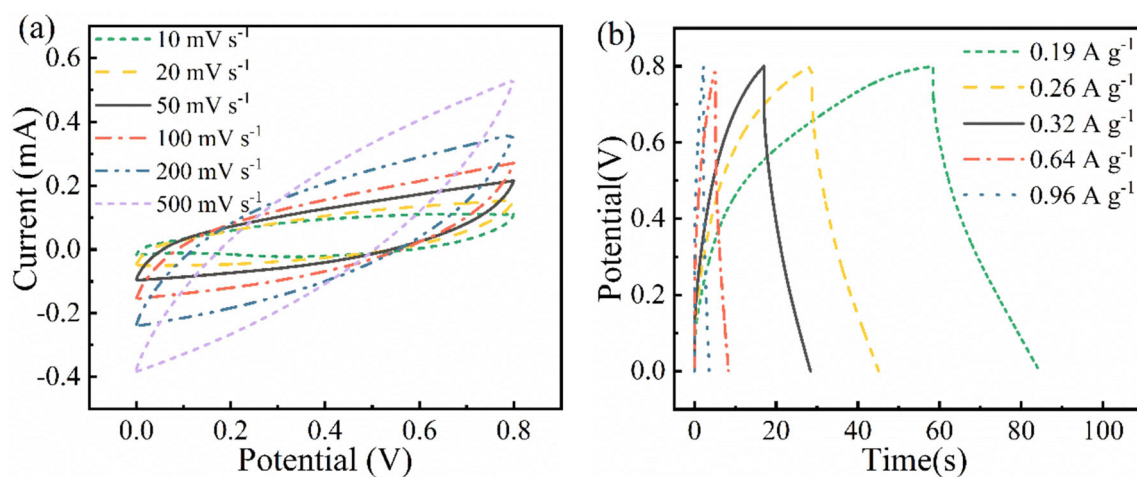


Fig. 6 **a** CV curves and **b** GCD curves of screen-printed fabric-based supercapacitor

Table 3 Comparison of the capacitance of flexible supercapacitor produced in this work with other flexible fabric/paper/membrane-based supercapacitors composed of carbon nanotubes

Substrate	Active materials	Technique	Gravimetric capacitance	Areal capacitance	References
Kapton polyimide	SWCNTs	Direct ink writing (DIW)	1.9 F g ⁻¹ at 1.32 A cm ⁻³	1.68 mF cm ⁻² at 1.32 A cm ⁻³	[15]
Polyethylene-terephthalate (PET)	SWCNTs	Spray coating	11 F g ⁻¹ at 5 mA cm ⁻²	N/A	[52]
Indium Tin Oxides (ITO)-coated PET film	MWCNTs	Injected drop-by-drop	41 F g ⁻¹ at 0.1 V s ⁻¹	N/A	[53]
PET	Functionalized MWCNTs	Spray coating	N/A	2.54 mF cm ⁻² at 10 mV s ⁻¹	[41]
Textiles	MWCNTs	3D printing	N/A	26.42 mF cm ⁻² at 0.42 mA cm ⁻²	[13]
Cotton fabric	SWCNTs	Dip coating	70 F g ⁻¹ at 10 μA g ⁻¹	N/A	[37]
Woven fabric	MWCNTs	Dip-pad-dry	8.35 F g ⁻¹ at 5 mV s ⁻¹	9.18mF cm ⁻² at 5 mV s ⁻¹	[32]
Non-woven cloth	Functionalized MWCNTs	Dip coating	N/A	16.40 mF cm ⁻² at 1 mA cm ⁻²	[17]
Cotton fabric	MWCNTs	Screen printing	26.4 F g ⁻¹ at 10 mV s ⁻¹ ; 6.2 F g ⁻¹ at 0.19 A g ⁻¹	13.8 mF cm ⁻² at 10 mV s ⁻¹ ; 3.3 mF cm ⁻² at 0.19 A g ⁻¹	This work

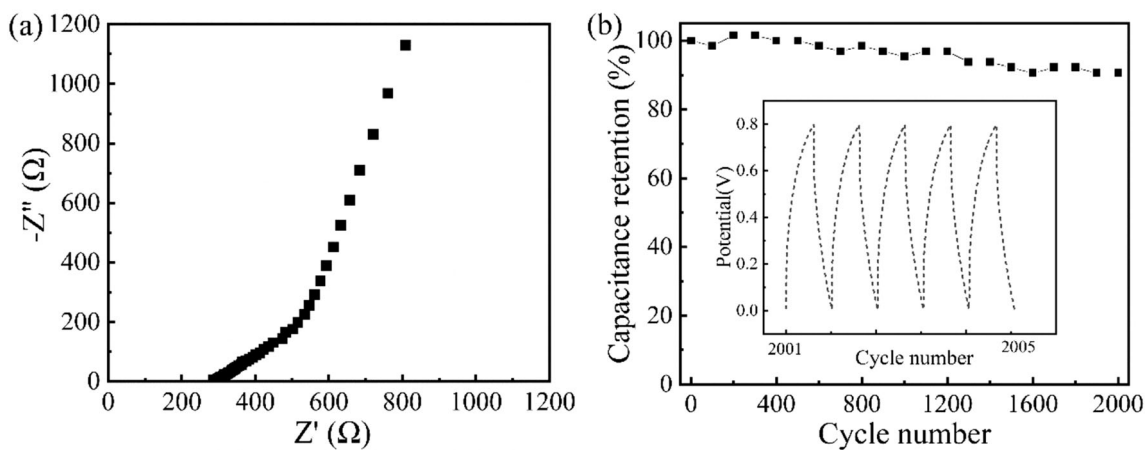


Fig. 7 **a** Nyquist plot and **b** cycling performance at current density of 0.64 A g⁻¹ of screen-printed fabric-based supercapacitor

indicating great cycle stability of fabricated supercapacitors.

3.5 The flexibility of fabric-based coplanar supercapacitor

The flexibility of fabric supercapacitors is essential for wearable application, because bending, twisting, and stretching movements often occur under wearing condition. In most researches [58–60], the flexibility of

supercapacitors was evaluated by bending the device to a certain degree. However, this flexibility test actually evaluates the static bending performance of flexible supercapacitor, which cannot completely represent the actual working performance of supercapacitors under wear [61]. In addition, a few of works evaluated the flexibility of energy storage device under dynamically bending. Nevertheless, they performed the test under relatively low strain rates (60 s per bending cycle[35] or strain rate of 2.1%

s^{-1} [36]), which obviously departure from the reality of human movements. Therefore, considering the wearing condition of wearable electronics, we performed the CV and GCD measurements for screen-printed fabric-based supercapacitor under dynamically bending-releasing cycles with relatively high strain rate of $20\% s^{-1}$ (3 s per bending cycle). Figure 8a shows the CV curves of fabric-based supercapacitor under initial state and dynamic bending state at scan rates of 20 to $100 mV s^{-1}$. It can be seen that there is no significant change in the CV curve at different scan rates, especially at relatively high scan rates of 50 and $100 mV s^{-1}$.

The GCD curves of supercapacitors under dynamically bending and initial state at different current densities are shown in Fig. 8b. It can be observed that the charge and discharge process of supercapacitor under dynamic bending is a little longer than that under initial state. This mainly attributed to the result of “mechanical-electrochemical synergy activation”. [62] The electrolyte ions tend to adjust with cycling to fully access the active electrode material under dynamic bending-releasing process. [62] Besides, the better contacting of electrodes and polymer gel electrolytes gives easier access to the electrolyte ions to permeate into the inner electrode materials. [36] Therefore, more active electrode materials can be utilized to form EDLC, and the specific capacitance and charging/discharging time of fabric-based supercapacitor increased slightly under dynamically bending-releasing.

4 Conclusion

In conclusion, the flexible fabric-based supercapacitor with coplanar integrated MWCNTs/textile electrode and current collectors was successfully fabricated by screen printing with cost-effective MWCNTs ink. Through the optimization of MWCNTs ink, the screen-printed fabric electrodes have excellent electrical and electrochemical performance. And the uniform and porous conductive network formed by carbon nanotubes is beneficial to charge transfer and ions absorption, which enables it to serve as integrated electrode and current collector in supercapacitor. Meanwhile, the screen-printed fabric-based supercapacitor showed great EDLC capacitive behavior and reversibility, and the gravimetric specific capacitance reached to $26.4 F g^{-1}$ at scan rate of $10 mV s^{-1}$. Most importantly, the excellent electrochemical performance could be maintained under dynamically bending-releasing cycles with high strain rate. These results validated the great flexibility and stability of fabricated coplanar textile-based supercapacitor. The successful integration of electrode and current collector greatly simplified the preparation process and structure of flexible supercapacitors, and provided a significant example for large-scale fabrication of flexible MWCNTs supercapacitors.

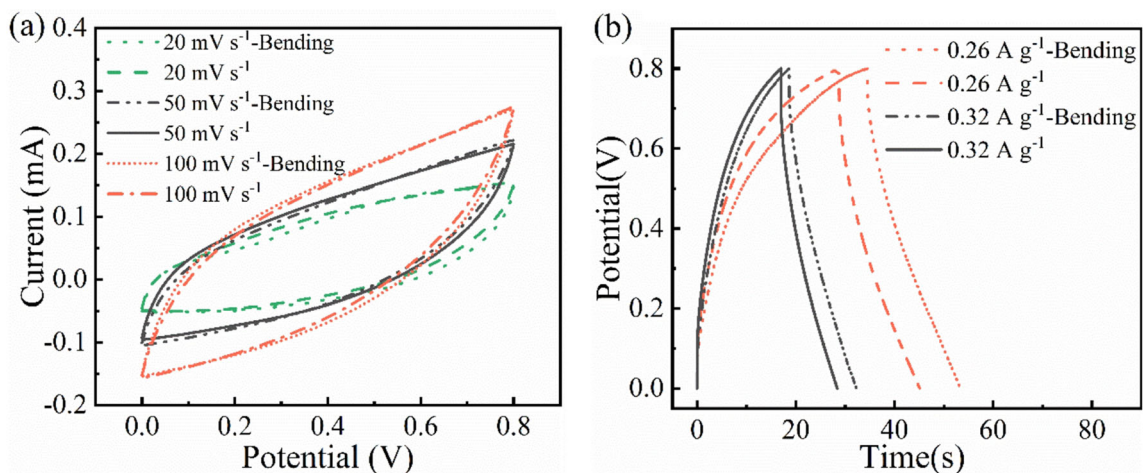


Fig. 8 **a** CV curves and **b** GCD curves of screen-printed coplanar fabric-based supercapacitor under initial state and dynamic bending-releasing cycles

Acknowledgements

This research was funded by the Natural Science Foundation of Shanghai (20ZR1400500) and the Fundamental Research Funds for the Central Universities (2232021G-01).

Author contributions

LJ: Methodology, validation, formal analysis, investigation, writing—original draft, writing—review and editing. HH: Investigation, methodology, writing—review and editing. JH: Investigation, formal analysis, supervision, writing—review and editing. XY: Investigation, supervision.

Data availability

The datasets generated during and/or analyzed during the current study are available from the corresponding author on reasonable request.

Declarations

Conflict of interest The authors declare that they have no known competing financial interests or personal relationships that could have appeared to influence the work reported in this paper.

References

- N. Karim, S. Afroj, S.R. Tan, P. He, A. Fernando, C. Carr, K.S. Novoselov, Scalable production of graphene-based wearable E-textiles. *ACS Nano* **11**, 12266–12275 (2017). <https://doi.org/10.1021/acsnano7b05921>
- P.M. Pataniya, C.K. Sumesh, M. Tannarana, C.K. Zankat, G.K. Solanki, K.D. Patel, V.M. Pathak, Flexible paper based piezo-resistive sensor functionalised by 2D-WSe₂-nanosheets. *Nanotechnology* (2020). <https://doi.org/10.1088/1361-6528/aba4cd>
- P.M. Pataniya, S.A. Bhakhar, M. Tannarana, C. Zankat, V. Patel, G.K. Solanki, K.D. Patel, P.K. Jha, D.J. Late, C.K. Sumesh, Highly sensitive and flexible pressure sensor based on two-dimensional MoSe₂ nanosheets for online wrist pulse monitoring. *J. Colloid Interface Sci.* **584**, 495–504 (2021). <https://doi.org/10.1016/j.jcis.2020.10.006>
- E. Heo, K.Y. Choi, J. Kim, J.H. Park, H. Lee, A wearable textile antenna for wireless power transfer by magnetic resonance. *Text. Res. J.* **88**, 913–921 (2018). <https://doi.org/10.1177/0040517517690626>
- H. Hong, J. Hu, X. Yan, UV curable conductive ink for the fabrication of textile-based conductive circuits and wearable UHF RFID tags. *ACS Appl. Mater. Interfaces* **11**, 27318–27326 (2019). <https://doi.org/10.1021/acsami.9b06432>
- W.L. Song, L.Z. Fan, Z.L. Hou, K.L. Zhang, Y.B. Ma, M.S. Cao, A wearable microwave absorption cloth. *J. Mater. Chem. C* **5**, 2432–2441 (2017). <https://doi.org/10.1039/c6tc05577j>
- R. Bellisle, C. Bjune, D. Newman, Ieee, Considerations for wearable sensors to monitor physical performance during spaceflight intravehicular activities, 42nd Annual International Conferences of the Ieee Engineering in Medicine and Biology Society: Enabling Innovative Technologies for Global Healthcare Embe'20, (Ieee, New York, 2020) pp. 4160–4164
- Y. Zhang, H.X. Mei, Y. Cao, X.H. Yan, J. Yan, H.L. Gao, H.W. Luo, S.W. Wang, X.D. Jia, L. Kachalova, J. Yang, S.C. Xue, C.G. Zhou, L.X. Wang, Y.H. Gui, Recent advances and challenges of electrode materials for flexible supercapacitors. *Coord. Chem. Rev.* **438**, 30 (2021). <https://doi.org/10.1016/j.ccr.2021.213910>
- S. Palchoudhury, K. Ramasamy, R.K. Gupta, A. Gupta, Flexible supercapacitors: a materials perspective. *Front. Mater.* **5**, 9 (2019). <https://doi.org/10.3389/fmats.2018.00083>
- P.C. Chen, H.T. Chen, J. Qiu, C.W. Zhou, Inkjet printing of single-walled carbon nanotube/RuO₂ nanowire supercapacitors on cloth fabrics and flexible substrates. *Nano Res.* **3**, 594–603 (2010). <https://doi.org/10.1007/s12274-010-0020-x>
- H. Park, J.W. Kim, S.Y. Hong, G. Lee, H. Lee, C. Song, K. Keum, Y.R. Jeong, S.W. Jin, D.S. Kim, J.S. Ha, Dynamically stretchable supercapacitor for powering an integrated biosensor in an all-in-one textile system. *ACS Nano* **13**, 10469–10480 (2019). <https://doi.org/10.1021/acsnano9b04340>
- X. Cui, J.Y. Tian, C.Y. Zhang, R. Cai, J. Ma, Z.K. Yang, Q.S. Meng, Comparative study of nanocarbon-based flexible multifunctional composite electrodes. *ACS Omega* **6**, 2526–2541 (2021). <https://doi.org/10.1021/acsomega0c04313>
- M.C. Zhang, M.Y. Zhao, M.Q. Jian, C.Y. Wang, Af. Yu, Z. Yin, X.P. Liang, H.M. Wang, K.L. Xia, X. Liang, J.Y. Zhai, Y.Y. Zhang, Printable smart pattern for multifunctional energy-management E-textile. *Matter* **1**, 168–179 (2019). <https://doi.org/10.1016/j.matt.2019.02.003>
- K.H. Choi, J. Yoo, C.K. Lee, S.Y. Lee, All-inkjet-printed, solid-state flexible supercapacitors on paper. *Energy Environ. Sci.* **9**, 2812–2821 (2016). <https://doi.org/10.1039/c6ee00966b>

15. B.L. Chen, Y.Z. Jiang, X.H. Tang, Y.Y. Pan, S. Hu, Fully packaged carbon nanotube supercapacitors by direct ink writing on flexible substrates. *ACS Appl. Mater. Interfaces* **9**, 28433–28440 (2017). <https://doi.org/10.1021/acsami7b06804>
16. A.M. Gaikwad, A.C. Arias, D.A. Steingart, Recent progress on printed flexible batteries: mechanical challenges, printing technologies, and future prospects. *Energy Technol.* **3**, 305–328 (2015). <https://doi.org/10.1002/ente.201402182>
17. J. Xu, H. Wu, C. Xu, H.T. Huang, L.F. Lu, G.Q. Ding, H.L. Wang, D.F. Liu, G.Z. Shen, D.D. Li, X.Y. Chen, Structural engineering for high energy and voltage output supercapacitors. *Chem. Eur. J.* **19**, 6451–6458 (2013). <https://doi.org/10.1002/chem.201204571>
18. Y.Z. Zhang, Y. Wang, T. Cheng, L.Q. Yao, X.C. Li, W.Y. Lai, W. Huang, Printed supercapacitors: materials, printing and applications. *Chem. Soc. Rev.* **48**, 3229–3264 (2019). <https://doi.org/10.1039/c7cs00819h>
19. D.P. Qi, Y. Liu, Z.Y. Liu, L. Zhang, X.D. Chen, Design of architectures and materials in in-plane micro-supercapacitors: current status and future challenges. *Adv. Mater.* **29**, 19 (2017). <https://doi.org/10.1002/adma.201602802>
20. F. Bu, W.W. Zhou, Y.H. Xu, Y. Du, C. Guan, W. Huang, Recent developments of advanced micro-supercapacitors: design, fabrication and applications. *NPJ Flex. Electron.* **4**, 16 (2020). <https://doi.org/10.1038/s41528-020-00093-6>
21. J. Liang, C.Z. Jiang, W. Wu, Printed flexible supercapacitor: Ink formulation, printable electrode materials and applications. *Appl. Phys. Rev.* **8**, 22 (2021). <https://doi.org/10.1063/5.0048446>
22. T.T. Huang, W.Z. Wu, Scalable nanomanufacturing of inkjet-printed wearable energy storage devices. *J. Mater. Chem. A* **7**, 23280–23300 (2019). <https://doi.org/10.1039/c9ta05239a>
23. D.B. Liu, K. Ni, J.L. Ye, J. Xie, Y.W. Zhu, L. Song, Tailoring the structure of carbon nanomaterials toward high-end energy applications. *Adv. Mater.* **30**, 13 (2018). <https://doi.org/10.1002/adma.201802104>
24. P. Xie, W. Yuan, X.B. Liu, Y.M. Peng, Y.H. Yin, Y.S. Li, Z.P. Wu, Advanced carbon nanomaterials for state-of-the-art flexible supercapacitors. *Energy Storage Mater.* **36**, 56–76 (2021). <https://doi.org/10.1016/j.jensm.2020.12.011>
25. X. Wu, M.Q. Zhang, T. Song, H.Y. Mou, Z.Y. Xiang, H.S. Qi, Highly durable and flexible paper electrode with a dual fiber matrix structure for high-performance supercapacitors. *ACS Appl. Mater. Interfaces* **12**, 13096–13106 (2020). <https://doi.org/10.1021/acsami9b19347>
26. A. Thess, R. Lee, P. Nikolaev, H.J. Dai, P. Petit, J. Robert, C.H. Xu, Y.H. Lee, S.G. Kim, A.G. Rinzler, D.T. Colbert, G.E. Scuseria, D. Tomanek, J.E. Fischer, R.E. Smalley, Crystalline ropes of metallic carbon nanotubes. *Science* **273**, 483–487 (1996). <https://doi.org/10.1126/science.2735274483>
27. Z. Liu, F. Mo, H. Li, M. Zhu, Z. Wang, G. Liang, C. Zhi, Advances in flexible and wearable energy-storage textiles. *Small Methods* **2**, 1800124 (2018). <https://doi.org/10.1002/smt.201800124>
28. M. Kaempgen, C.K. Chan, J. Ma, Y. Cui, G. Gruner, Printable thin film supercapacitors using single-walled carbon nanotubes. *Nano Lett.* **9**, 1872–1876 (2009). <https://doi.org/10.1021/nl8038579>
29. L.B. Hu, M. Pasta, F. La Mantia, L.F. Cui, S. Jeong, H.D. Deshazer, J.W. Choi, S.M. Han, Y. Cui, Stretchable, porous, and conductive energy textiles. *Nano Lett.* **10**, 708–714 (2010). <https://doi.org/10.1021/nl903949m>
30. P. Forouzandeh, V. Kumaravel, S.C. Pillai, Electrode materials for supercapacitors: a review of recent advances. *Catalysts* **10**, 72 (2020). <https://doi.org/10.3390/catal10090969>
31. T. Tao, S.G. Lu, Y. Chen, A review of advanced flexible lithium-ion batteries. *Adv. Mater. Technol.* (2018). <https://doi.org/10.1002/admt.201700375>
32. R.S. Costa, A. Guedes, A.M. Pereira, C. Pereira, Fabrication of all-solid-state textile supercapacitors based on industrial-grade multi-walled carbon nanotubes for enhanced energy storage. *J. Mater. Sci.* **55**, 10121–10141 (2020). <https://doi.org/10.1007/s10853-020-04709-0>
33. L.H. Jiang, H. Hong, X. Yan, J.Y. Hu, Facile thermoplastic polyurethane-based multi-walled carbon nanotube ink for fabrication of screen-printed fabric electrodes of wearable e-textiles with high adhesion and resistance stability under large deformation. *Text. Res. J.* (2021). <https://doi.org/10.1177/00405175211008613>
34. M.Y. Lin, Y.Z. Gai, D. Xiao, H.J. Tan, Y.P. Zhao, Preparation of pristine graphene paste for screen printing patterns with high conductivity. *Chem. Phys. Lett.* **713**, 98–104 (2018). <https://doi.org/10.1016/j.cpl.2018.10.022>
35. S.G. Woo, S. Yoo, S.H. Lim, J.S. Yu, K. Kim, J.G. Lee, D.G. Lee, J.H. Kim, S.Y. Lee, Galvanically replaced, single-bodied lithium-ion battery fabric electrodes. *Adv. Funct. Mater.* **30**, 9 (2020). <https://doi.org/10.1002/adfm.201908633>
36. X. Li, T.L. Gu, B.Q. Wei, Dynamic and galvanic stability of stretchable supercapacitors. *Nano Lett.* **12**, 6366–6371 (2012). <https://doi.org/10.1021/nl303631e>
37. M. Pasta, F. La Mantia, L.B. Hu, H.D. Deshazer, Y. Cui, Aqueous supercapacitors on conductive cotton. *Nano Res.* **3**, 452–458 (2010). <https://doi.org/10.1007/s12274-010-0006-8>
38. T.G. Yun, M. Oh, L.B. Hu, S. Hyun, S.M. Han, Enhancement of electrochemical performance of textile based supercapacitor using mechanical pre-straining. *J. Power Sources* **244**, 783–791 (2013). <https://doi.org/10.1016/j.jpowsour.2013.02.087>
39. M.S. Sadi, M.Y. Yang, L. Luo, D.S. Cheng, G.M. Cai, X. Wang, Direct screen printing of single-faced conductive

- cotton fabrics for strain sensing, electrical heating and color changing. *Cellulose* **26**, 6179–6188 (2019). <https://doi.org/10.1007/s10570-019-02526-6>
40. T.Q. Hao, W. Wang, D. Yu, A flexible cotton-based supercapacitor electrode with high stability prepared by multi-walled CNTs/PANI. *J. Electron. Mater.* **47**, 4108–4115 (2018). <https://doi.org/10.1007/s11664-018-6306-6>
 41. J. Yun, D. Kim, G. Lee, J.S. Ha, All-solid-state flexible micro-supercapacitor arrays with patterned graphene/MWNT electrodes. *Carbon* **79**, 156–164 (2014). <https://doi.org/10.1016/j.carbon.2014.07.055>
 42. T. Fischer, J. Ruhling, N. Wetzold, T. Zillger, T. Weissbach, T. Goschel, M. Wurfel, A. Hubler, L. Kroll, Roll-to-roll printed carbon nanotubes on textile substrates as a heating layer in fiber-reinforced epoxy composites. *J. Appl. Polym. Sci.* **135**, 6 (2018). <https://doi.org/10.1002/app.45950>
 43. J.Q. Qi, Y.W. Chen, Q. Li, Y.W. Sui, Y.Z. He, Q.K. Meng, F.X. Wei, Y.J. Ren, J.L. Liu, Hierarchical NiCo layered double hydroxide on reduced graphene oxide-coated commercial conductive textile for flexible high-performance asymmetric supercapacitors. *J. Power Sources* (2020). <https://doi.org/10.1016/j.jpowsour.2019.227342>
 44. S.L. Zhang, N. Pan, S.P. Evaluation, *Adv. Energy Mater.* **5**, 19 (2015). <https://doi.org/10.1002/aenm.201401401>
 45. W.M. Haynes, *CRC Handbook of Chemistry and Physics*, 95th edn. (Taylor and Francis, CRC Press, Boca Raton, 2014), pp. 2117–2119. <https://doi.org/10.1201/b17118>
 46. F. Beguin, V. Presser, A. Balducci, E. Frackowiak, Carbons and electrolytes for advanced supercapacitors. *Adv. Mater.* **26**, 2219–2251 (2014). <https://doi.org/10.1002/adma.201304137>
 47. M. Noked, E. Avraham, Y. Bohadana, A. Soffer, D. Aurbach, Development of anion stereoselective, activated carbon molecular sieve electrodes prepared by chemical vapor deposition. *J. Phys. Chem. C* **113**, 7316–7321 (2009). <https://doi.org/10.1021/jp811283b>
 48. C.C. Wan, Y. Jiao, J. Li, Flexible, highly conductive, and free-standing reduced graphene oxide/polypyrrole/cellulose hybrid papers for supercapacitor electrodes. *J. Mater. Chem. A* **5**, 3819–3831 (2017). <https://doi.org/10.1039/c6ta04844g>
 49. J. Xu, D.X. Wang, Y. Yuan, W. Wei, L.L. Duan, L.X. Wang, H.F. Bao, W.L. Xu, Polypyrrole/reduced graphene oxide coated fabric electrodes for supercapacitor application. *Org. Electron.* **24**, 153–159 (2015). <https://doi.org/10.1016/j.orgel.2015.05.037>
 50. X.L. Li, R. Liu, C.Y. Xu, Y. Bai, X.M. Zhou, Y.J. Wang, G.H. Yuan, High-performance polypyrrole/graphene/SnCl₂ modified polyester textile electrodes and yarn electrodes for wearable energy storage. *Adv. Funct. Mater.* (2018). <https://doi.org/10.1002/adfm.201800064>
 51. B.A. Mei, O. Munteshari, J. Lau, B. Dunn, L. Pilon, Physical interpretations of nyquist plots for EDLC electrodes and devices. *J. Phys. Chem. C* **122**, 194–206 (2018). <https://doi.org/10.1021/acs.jpcc.7b10582>
 52. H.Y. Gan, C.H. Chua, S.M. Chan, B.K. Lok, *Performance Characterization of Flexible Printed Supercapacitors* (IEEE, New York, 2009). <https://doi.org/10.1109/eptc.2009.5416532>
 53. F. Markoulidis, C. Lei, C. Lekakou, Fabrication of high-performance supercapacitors based on transversely oriented carbon nanotubes. *Appl. Phys. A: Mater. Sci. Process.* **111**, 227–236 (2013). <https://doi.org/10.1007/s00339-012-7471-8>
 54. H.H. Zhang, Y. Qiao, Z.S. Lu, Fully printed ultraflexible supercapacitor supported by a single-textile substrate. *ACS Appl. Mater. Interfaces* **8**, 32317–32323 (2016). <https://doi.org/10.1021/acsami.6b11172>
 55. H.L. Dai, G.X. Zhang, D. Rawach, C.Y. Fu, C. Wang, X.H. Liu, M. Dubois, C. Lai, S.H. Sun, Polymer gel electrolytes for flexible supercapacitors: Recent progress, challenges, and perspectives. *Energy Storage Mater.* **34**, 320–355 (2021). <https://doi.org/10.1016/j.jensm.202009018>
 56. S.Q. Li, Z.Y. Fan, Nitrogen-doped carbon mesh from pyrolysis of cotton in ammonia as binder-free electrodes of supercapacitors. *Microporous Mesoporous Mater.* **274**, 313–317 (2019). <https://doi.org/10.1016/j.micromeso.201809002>
 57. L. Liu, Q.Y. Tian, W.J. Yao, M.X. Li, Y.W. Li, W. Wu, All-printed ultraflexible and stretchable asymmetric in-plane solid-state supercapacitors (ASCs) for wearable electronics. *J. Power Sources* **397**, 59–67 (2018). <https://doi.org/10.1016/j.jpowsour.201807013>
 58. X. Pu, L.X. Li, H.Q. Song, C.H. Du, Z.F. Zhao, C.Y. Jiang, G.Z. Cao, W.G. Hu, Z.L. Wang, A self-charging power unit by integration of a textile triboelectric nanogenerator and a flexible lithium-ion battery for wearable electronics. *Adv. Mater.* **27**, 2472–2478 (2015). <https://doi.org/10.1002/adma.201500311>
 59. L.L. Xu, M.X. Guo, S. Liu, S.W. Bian, Graphene/cotton composite fabrics as flexible electrode materials for electrochemical capacitors. *RSC Adv.* **5**, 25244–25249 (2015). <https://doi.org/10.1039/c4ra16063k>
 60. N. Keawploy, R. Venkatkarthick, P. Wangyao, X.Y. Zhang, R.P. Liu, J.Q. Qin, Eco-friendly conductive cotton-based textile electrodes using silver- and carbon-coated fabrics for advanced flexible supercapacitors. *Energy Fuels* **34**, 8977–8986 (2020). <https://doi.org/10.1021/acs.energyfuels.0c01419>
 61. L.Y. Yuan, X.H. Lu, X. Xiao, T. Zhai, J.J. Dai, F.C. Zhang, B. Hu, X. Wang, L. Gong, J. Chen, C.G. Hu, Y.X. Tong, J. Zhou, Z.L. Wang, Flexible solid-state supercapacitors based on

- carbon nanoparticles/mno₂ nanorods hybrid structure. ACS Nano **6**, 656–661 (2012). <https://doi.org/10.1021/nn2041279>
62. T.L. Gu, B.Q. Wei, Fast and stable redox reactions of MnO₂/CNT hybrid electrodes for dynamically stretchable pseudocapacitors. Nanoscale **7**, 11626–11632 (2015). <https://doi.org/10.1039/c5nr02310f>

Publisher's Note Springer Nature remains neutral with regard to jurisdictional claims in published maps and institutional affiliations.